



Published in final edited form as:

Mater Sci Eng C Mater Biol Appl. 2020 May ; 110: . doi:10.1016/j.msec.2020.110656.

Subcutaneous priming of protein-functionalized chitosan scaffolds improves function following spinal cord injury

Trevor R Ham^a, Dipak D Pukale^b, Mohammad Hamrangsekachae^a, Nic D Leipzig^{a,b}

^aDepartment of Biomedical Engineering, University of Akron, Akron, OH, 44325

^bDepartment of Chemical and Biomolecular Engineering, University of Akron, Akron, OH, 44325

Abstract

Strategies using neural stem cells (NSCs) to aid regeneration following spinal cord injury (SCI) show much promise, but challenges remain regarding implementation and efficacy. In this work, we explored the use of an NSC-seeded scaffold consisting of covalently immobilized interferon- γ and rat NSCs within a hydrogel matrix (methacrylamide chitosan). We placed the scaffolds within the subcutaneous environment of rats, allowing them to incubate for 4 weeks in order to prime them for regeneration prior to being transplanted into a right lateral hemisection SCI model in the same animal. We found that subcutaneous priming reduced the lineage commitment of encapsulated NSCs, as observed by increased nestin expression and decreased NeuN expression. When combined with intracellular σ peptide administration (which reduces inhibition from the glial scar), subcutaneous maturation improved functional outcomes, which were assessed by BBB score and quantitative gait parameters (fore and hind limb duty factor imbalance, right and left paw placement accuracy). Although we did not observe any direct reconnection of the transplanted cells with the host tissue, we did observe neurofilament fibers extending from the host tissue into the scaffold. Importantly, the mechanism for improved functional outcomes is likely an increase in trophic support from subcutaneously maturing the scaffold, which is enhanced by the administration of ISP.

Keywords

Neural stem cells; spinal cord injury; gait analysis; intracellular σ peptide; tissue engineering

1. Introduction

Following traumatic spinal cord injury (SCI), a permanent disruption in the arrangement, type, and number of cells at the injury site drives sensory and motor deficits.^[1] Importantly, the endogenous repair response fails to generate any new neurons and functional losses below the damaged region persist indefinitely.^[2] This is exacerbated by a variety of secondary injury processes, including the formation of a glial scar which surrounds the

Publisher's Disclaimer: This is a PDF file of an unedited manuscript that has been accepted for publication. As a service to our customers we are providing this early version of the manuscript. The manuscript will undergo copyediting, typesetting, and review of the resulting proof before it is published in its final form. Please note that during the production process errors may be discovered which could affect the content, and all legal disclaimers that apply to the journal pertain.

primary lesion and restricts growth of endogenous axons into the lesion cavity.^[3] The goal of SCI therapies is to restore function to the patient. This may be accomplished through strategies that take advantage of the remaining neural circuits (e.g., locomotor training^[4, 5] and/or epidural stimulation^[6, 7]) or reduce the inhibitory microenvironment which restricts host axonal regrowth (e.g., intracellular σ peptide, ISP,^[8] a membrane-permeable mimic of the protein tyrosine phosphatase σ wedge domain, which relieves chondroitin sulfate proteoglycan-mediated inhibition.). However, in moderate to severe cases of SCI, these approaches fail to fully restore function to pre-injury levels.

Due to the insufficient host cellular response, delivering exogenous neural stem cells (NSCs) is a promising strategy to restore function through the generation of new cell populations and neuronal connections.^[9] NSC grafts have shown great promise to provide local trophic support^[10] or extend processes into the host tissue^[11] over remarkable distances (25 mm).^[12] Despite these promising findings, a treatment that effectively guides the behavior of NSCs to functionally regenerate and replace damaged tissue is elusive. We previously proposed that this could be accomplished via guided neuronal lineage specification from NSCs exposed to immobilized interferon- γ (IFN- γ , which is neurogenic).^[13, 14] We immobilized IFN- γ to methacrylamide chitosan (MAC, which forms a photocrosslinkable and cell-supportive hydrogel^[15]) and formed NSC-seeded scaffolds by mixing IFN- γ immobilized-MAC with photoreactive laminin (to allow NSCs to interact with MAC) and NSCs.^[16] We chose MAC because, in addition to being photocrosslinkable, it allows for the facile attachment of functional groups at primary amines and is similar in structure to hyaluronan, a component of native spinal cord extracellular matrix.^[13] However, we found that this approach, when applied directly to the spinal cord immediately following injury, did not result in improved function.^[16] Considering that NSC grafts show improved tissue-level integration after extended periods of maturation in the spinal cord,^[17] and maturing tissue grafts in the subcutaneous environment has been used to develop grafts in other tissues,^[18] we investigated the approach of subcutaneously maturing spinal cord grafts. We have found that maturing NSC-seeded scaffolds in the subcutaneous environment for 4 wks resulted in the expression of regionally appropriate,^[19] CNS-specific developmental markers.^[20] This led us to propose a treatment paradigm wherein NSC-seeded scaffolds, formed from MAC and containing covalently immobilized IFN- γ , could be primed for regeneration via maturation in the subcutaneous environment prior to transplantation into an injured spinal cord.

Here, we present an investigation of this approach to treat a subacute (2 wks post-injury) T10 right lateral hemisection in rats (Figure 1). This injury model was chosen as the most straightforward model to accommodate a biomaterial scaffold and to allow for comparison with previous work.^[16, 21] We applied these scaffolds to the injury site and evaluated locomotor recovery via BBB score and an open source, quantitative gait analysis technique (GAITOR^[22, 23]). We confirmed our findings by examining retrograde tracer uptake. Finally, we provided insights into the tissue-level integration of the graft and spinal cord by investigating the amount of remaining implanted cells, their lineage distribution, and whether or not host axons were able to extend from the remaining tissue into the scaffold.

2. Results

2.1. Functional data show benefits of subcutaneously maturing NSC-seeded scaffolds

Given the chaotic cell response to SCI, using tissue engineering/regenerative medicine to generate new neuronal connections and guide cell behavior along pro-regenerative pathways is an important goal. Our previous work has shown that immobilized IFN- γ stimulates neuronal differentiation of NSCs;^[13, 14, 20, 24, 25, 26] however, we found that application of NSC-seeded scaffolds formed from MAC with immobilized IFN- γ directly to the spinal cord without any maturation failed to generate functional improvements.^[16] Furthermore, subcutaneously maturing these NSC-seeded scaffolds with immobilized IFN- γ may prime them for regeneration.^[20] Lastly, reducing inhibition from the glial scar contributes to functional recovery^[8] by enabling the regeneration of host axons. Thus, we sought to combine these two ideas (subcutaneous maturation and ISP administration) and test this approach in a rat hemisection model of SCI. Our hypothesis was that subcutaneously maturing NSC-seeded scaffolds while reducing inhibitory cues from the surrounding scar (via ISP) would improve locomotor function over time. We evaluated this hypothesis along two scientific, testable questions: first, does subcutaneous maturation (SubQ) improve locomotor function compared to a no treatment control, and second, is this improved by ISP?

A repeated measures ANOVA of the BBB scores (Figure 2 shows NSC-seeded scaffolds, see Figure A.8 for control groups) reveals interesting contributions from each factor (see section 5.15 for the full experimental design and analysis): on their own, NSCs ($p < 0.0001$) and ISP ($p = 0.0004$) were significant, but SubQ ($p = 0.982$) was not. This makes sense, as we expected that maturing the scaffolds subcutaneously would have an effect on the NSCs, not the scaffold material itself. Indeed, this is supported by the data: NSCs*SubQ ($p = 0.0005$) was significant. Additionally, NSCs*SubQ*ISP was significant ($p = 0.0224$), suggesting that there is a benefit to combining all the factors together.

We found that combining subcutaneously matured NSC-seeded scaffolds with ISP administration improved BBB scores vs. a no treatment control (Figure 2), beginning at wk 6. In fact, it was the only treatment that we studied to do so. Comparing the effects of subcutaneous maturation with and without ISP administration yields interesting observations. First, maturing an empty scaffold within the subcutaneous environment imparts no benefits beyond a normal, non-matured scaffold (Figure A.8). Second, implementing subcutaneous maturation without ISP administration did yield some benefits, but these were not enough to be statistically significant ($p > 0.05$). Likewise, when administering ISP to an animal receiving an empty scaffold, it made no difference whether that scaffold was subcutaneously matured or not (Figure A.8).

The gait parameters measured via GAITOR illuminate some interesting underlying trends. Since our injury model affected right hindlimb locomotion, we studied how much time the animals spent on their right hindpaw vs. left (hindlimb duty factor imbalance, Figure 3B), and how accurately they could place their right hindpaw (right paw placement accuracy, Figure 3C). Figure 3 shows the results for the NSC-seeded scaffolds, while control groups can be found in Figure A.9. We found that, as expected, our injury caused all the rats to

spend more time on their left hindpaw (negative DF imbalance) and place their right hindpaw less accurately (positive residual). A repeated measures ANOVA of these parameters over time yields the following conclusions: for hindlimb duty factor imbalance, NSCs ($p < 0.0001$) and NSCs*SubQ*ISP ($p = 0.0384$) were significant. For right paw placement accuracy, NSCs ($p < 0.0001$), ISP ($p = 0.0147$), and NSCs*SubQ*ISP ($p = 0.0244$) were significant.

Comparing individual groups shows similar trends to BBB score, but with additional groups showing differences vs. the no treatment control. Without ISP administration, maturing NSC-scaffolds in the subcutaneous environment reduced hindlimb duty factor imbalance vs. negative control (Figure 3B) beginning at week 8. NSC-seeded scaffolds without subcutaneous maturation reduced imbalance, but not enough to be statistically different from the control ($p > 0.05$), indicating the role that the subcutaneous environment plays in improving the efficacy of this approach. Subcutaneous maturation had no effect on empty scaffolds, showing that the subcutaneous environment affects primarily NSCs, not the scaffold material (Figure A.9). Interestingly, with ISP administration, both types of NSC-seeded scaffolds (subcutaneously matured and not matured) reduced imbalance vs. the negative control, although subcutaneous maturation showed benefits at an earlier timepoint. The recovery of paw placement accuracy (Figure 3C) followed an interesting trend: without ISP administration, both types of NSC-seeded scaffolds improved accuracy, although again, subcutaneous maturation showed improvements more quickly. The tracing results show that at week 16, both groups receiving subcutaneously matured scaffolds (with and without ISP) were significantly different from the no treatment control (Figure A.11).

2.2. Subcutaneous maturation does not affect the number of remaining cells

We next sought to determine whether there was a difference in the number of surviving GFP+ cells remaining in the scaffold after 16 wks. We collected 10 μm longitudinal sections (from the top down) and counted the number of GFP+ cells in each. After taking the average across all sections, we found that there were no significant differences between the 4 NSC groups ($p > 0.05$, Figure 4). We also noticed that there was some heterogeneity in the number of GFP+ cells per section, as can be seen in Figure 4E and qualitatively in Figures 5 — 7. Additionally, we did not see substantial migration of GFP+ cells into the surrounding tissue, obvious reconnection, or GFP+ neurite extension into the host, as others have seen. [11, 12, 17, 27]

2.3. Subcutaneous maturation increases nestin expression and decreases NeuN expression

NSCs are known to increase host axon regrowth via secreted factors following SCI;^[9] this effect may be reduced as they differentiate into mature lineages.^[10] Thus, we sought to determine whether the improvements in function from subcutaneous maturation correlated with changes in mature (NeuN, Figure 5) vs. immature (nestin, Figure 6) marker expression. We found that subcutaneous maturation decreased the percentage of GFP+ cells expressing NeuN, a marker for neuronal nuclei ($p < 0.001$) from approx. 55% to 40% (Figure 5E). ISP had no effect on NeuN expression. We also observed some host (i.e., GFP-) NeuN+ cells within the scaffold, especially within the ISP groups (indicated by arrows in Figure 5A–D)

— this hints at a possible combination of trophic effects from subcutaneous maturation and ISP administration increasing host neuronal outgrowth into the scaffold. However, we did not see any evidence of robust reconnection spanning the entire length of the scaffold. Within the scaffold, the NeuN+ and GFP+ (or both) cells were not evenly distributed and tended to appear in clumps. We also did not see normal NeuN+ morphologies within the scaffolds, either from GFP+ or host cells. Figure 5G + I show the morphologies of NeuN+ cells within the scaffold in detail, while F + H show morphologies of NeuN+ cells within the spinal cord, bordering the lesion. We saw large amounts of NeuN+ cells with normal morphologies on the border of the scaffolds (in particular, Figure 5F), but where these cells appeared in the scaffold their morphology was much more compact. We did not see any RIP (a marker for oligodendrocytes) expression within the scaffold (data not shown).

We also found that subcutaneous maturation increased the percentage of GFP+ cells expressing nestin (a neural precursor marker) from approx. 20% to 30% (Figure 6E). Again, ISP had no effect. Interestingly, we also saw aligned nestin/GFP+ fibers running through the scaffold in the subQ+/ISP+/NSC+ group (arrows in I). As nestin is an immature marker, it is possible that at longer timepoints this phenomenon would become widespread and neuronal reconnection would emerge, as has been observed by others.^[17] This may contribute to the increased recovery observed in this group. We did occasionally observe similar fibers throughout the scaffolds in the other NSC groups, but they were neither as prominent nor as long, echoing the modest recovery observed in those groups in the gait and retrograde tracing analyses. Lastly, we saw pronounced ellipsoid clusters of nestin/GFP+ cells in both subQ+/NSC+ groups, with and without ISP. We have observed these before upon subcutaneous maturation of these scaffolds.^[20] They are reminiscent of neural tubes, a hallmark of early central nervous system development. We have previously investigated this finding in more detail and found that the cells also adopted a regionally-appropriate HOX expression profile^[19] which may relate to improved trophic support. Future studies will investigate the secretome of the NSCs within each scaffold and investigate the role of regional identity. As the secretome of undifferentiated NSCs provides trophic support to specific populations of host neurons,^[10] it is likely that the benefits of subcutaneous maturation were realized by increased trophic support to the proper host neurons, as evinced by the prevalence of nestin/GFP+ cell clusters in these groups.

2.4. Robust neurofilament expression at the periphery of the scaffold is augmented by subcutaneous maturation and ISP administration

Finally, we aimed to determine if any of the treatments affected integration of the scaffold with the host tissue (Figure 7). In all groups, we observed neurofilament (NF) expression within the scaffold near the tissue border. The NF+ fibers aligned themselves with the scaffold. In many cases (e.g., Figure 7A), the scaffold was not aligned with the orientation of the tissue, so neurite outgrowth changed direction at the scaffold/spinal cord border, highlighting the importance of scaffold alignment. Scaffold alignment did not affect functional outcomes, as there was no trend between different treatments. The microarchitecture of spinal cord scaffolds has been shown to influence axonal alignment,^[28, 29] as regrowing axons align strongly with channels inside spinal cord implants. This

influence of channels within our subcutaneously matured NSC-seeded scaffolds will be investigated in future studies.

3. Discussion

The focus of the current study was on evaluating a novel approach to combine different tissue engineering/regenerative medicine approaches and determine whether this approach would improve functional and histological outcome measures following a SCI in rats. We hypothesized that subcutaneously maturing NSC-seeded scaffolds while reducing inhibitory cues from the surrounding scar (via ISP) would improve locomotor function over time. Overall, the functional results (BBB score, gait analysis, and tracing) confirm our hypothesis, and point to a possible mechanism for recovery. In all functional tests, subcutaneously maturing NSC-seeded scaffolds while administering ISP improved outcomes vs. a negative control. However, examining retrograde tracer uptake and hindlimb duty factor imbalance (more sensitive measures) shows that implanting the same scaffolds without ISP improved outcomes as well. Additionally, paw placement accuracy indicated that even NSC-seeded scaffolds without SubQ or ISP improved outcomes. In short, for functional metrics, the introduction of NSCs into the scaffolds improved outcomes, subcutaneous maturation improved outcomes further, and adding ISP improved outcomes further still. We have previously investigated non-subcutaneously matured, NSC-seeded scaffolds in a similar injury model (administered acutely following T8 hemisection, without ISP administration).^[16] As here, we found that they did not improve BBB scores. However, they did improve histological outcomes. The addition of more sensitive functional outcomes in the present study provides further support for the notion that NSC-seeded scaffolds on their own, without subcutaneous maturation, provide a modest contribution towards functional regeneration. Altogether, the functional data suggested that they indirectly contributed to recovery, rather than directly differentiating into functional phenotypes and reconnecting damaged neural pathways. Additionally, as we didn't observe improvements until week 6, the mechanism is likely trophic, rather than protective, with each individual component (NSCs, SubQ, ISP) contributing support. Thus, we next wanted to examine the amount of GFP+ (exogenous) cells remaining within the lesion, their lineage distribution, and whether there was integration between the scaffold and surrounding tissue.

The histological outcome measures indicated a lack of migration and reconnection between the cells in the scaffold and the spinal cord. This finding may be due to the number of cells or our chosen timepoint — both variables will be studied in more detail in future experiments. Low tissue-level integration of implanted cells, coupled with the observed functional benefits, again provides evidence for an indirect contribution of our system to recovery. Since the number of remaining cells (along with, qualitatively, their distribution and morphology) did not vary between treatments, we next investigated whether there were phenotypical differences between GFP+ cells which were affected by subcutaneous maturation.

Together with the functional improvements and changes in phenotype from subcutaneous maturation, two findings further support the mechanism of indirect trophic support: first, groups with NSCs showed more robust NF expression within the scaffold than groups

without NSCs. Second, we did not observe substantial co-expression of NF and GFP within any of the scaffolds. NF expression within the scaffold was also enhanced by both subcutaneous maturation (in groups with NSCs) and ISP administration. This is similar to previous reports where ISP increased host neurofilament expression in a contusion injury model^[8] and provides additional evidence for the role of ISP as increasing the efficacy of trophic support provided by subcutaneously matured, NSC-seeded scaffolds. Indeed, if host axonal regeneration due to trophic effects from NSCs was primarily responsible for functional improvements, it stands to reason that ISP administration would improve this by reducing the inhibition from the glial scar surrounding the lesion. The benefits of combining multiple treatments together is a common finding within the SCI literature (e.g., the inclusion of locomotor training^[30] and epidural stimulation),^[6] and it appears likely that combinatorial approaches, rather than a single “magic bullet^[31]” therapy, will revolutionize clinical SCI treatment. Further modifications will need to be made to the current approach as it is investigated further and developed for clinical translation. Alternative sources of NSCs and adjustments to the timing of subcutaneous implantation will likely be critical steps. The development of a bank for organ donor human NSCs has begun and their safety has been demonstrated, including in SCI models.^[32, 33, 34] In addition, the implantation of tissue grafts into the subcutaneous space as an *in vivo* bioreactor has been applied clinically^[18] (e.g., craniotomy graft storage^[35, 36]).

Overall, it is becoming apparent that indirect trophic support is a major driver of benefits in many applications of stem cell therapy. This is prominent in the mesenchymal stem cell (MSC) literature, as MSCs have been shown to primarily improve function through influencing the microenvironment via secreted factors,^[37] rather than differentiating into mature, functional tissue (some have even suggested renaming MSCs as “medicinal signaling cells”).^[38] Our present study adds to this growing body of literature.

Functional regeneration via the trophic effects of unguided stem cell therapy is clearly sufficient for the regeneration of certain injuries,^[39] but SCI presents a unique challenge. Due to the limited innate capacity for regeneration in the adult CNS and the dense, complex nature of spinal cord microarchitecture, simply encouraging host regeneration is effective but unlikely to be enough. Indeed, as seen here, improving the trophic support of NSCs by subcutaneous maturation improved function but not to the level of healthy tissue (Figures A.8 and A.9). The surviving host cells will need to be directly augmented with functional, exogenous replacements, while a material scaffolding provides guidance and protection. Our observation of aligned nestin/GFP+ fibers within the scaffold, in addition to robust NF expression at the periphery, suggest that we can likely enhance the ability of this system to directly contribute to recovery by increasing the number of implanted cells, extending the recovery time, and adding locomotor training. The direct replacement of damaged tissue from NSCs may be within reach, and we can move closer to that goal by continuing to study new techniques for guiding NSC behavior, such as priming them for regeneration within the subcutaneous environment.

4. Conclusions

We found that maturing NSC-seeded scaffolds (formed from MAC and containing immobilized IFN- γ) within the subcutaneous environment improved locomotor function over a period of 16 weeks. A statistical analysis of various functional tests (BBB score, gait analysis, retrograde tracer uptake) indicated that NSCs, subcutaneous maturation, and the administration of ISP to reduce glial inhibition combined to improve recovery. Tissue-level examination via IHC indicated that recovery was likely accomplished through indirect, trophic support from NSCs. Subcutaneous maturation appeared to enhance this effect by encouraging delivered NSCs to remain undifferentiated (increased nestin and decreased NeuN expression) and assemble into neural tube-like clusters, while ISP reduced inhibition, allowing host axons to re-grow across the lesion (strong NF staining at the interface between scaffold and intact spinal cord). We found that the combination of subcutaneous maturation and ISP increased the prevalence of aligned nestin+ fibers from the implanted cells within the scaffold, indicating a potential avenue for direct integration of our scaffold with the intact cord.

5. Experimental Section

5.1. Isolation and culture of NSCs

All procedures involving animals were approved by the University of Akron Institutional Animal Care and Use Committee. We isolated NSCs from the subventricular zone of 7 wk old female GFP+ Fisher 344 rats (strain: F344-Tg(UBCEGFP)F455, Rat Resource and Research Center, University of Missouri) as previously described.^[13, 24] We expanded them in suspension culture using growth medium: neurobasal medium, 2 mM L-glutamine, 100 $\mu\text{g}/\text{mL}$ penicillin-streptomycin, B27 supplement (all Thermo Fisher Scientific), 20 ng/mL epidermal growth factor (Sigma-Aldrich), 20 ng/mL basic fibroblast growth factor (Peprotech), and 2 $\mu\text{g}/\text{mL}$ heparin (Sigma-Aldrich). We used passage 5 NSCs for scaffold formation.

5.2. Synthesis of scaffold components

We synthesized MAC^[13, 15, 24] using chitosan (Mycodex, 200 kDa, 84% deacetylation) and methacrylic anhydride (Sigma-Aldrich), and lyophilized (Labconco FreeZone 4.5) it before use. We then synthesized MAC-DIBO using dibenzocyclooctyne-N-hydroxysuccinimide ester (Click Chemistry Tools) as described in.^[13] We produced, extracted, and purified azide-tagged interferon- γ as previously described.^[13, 40, 41] We synthesized photo-reactive laminin as previously described^[20] to add CNS-specific attachment ligands.^[25] We prepared the photoinitiator solution by dissolving IRG-2959 (Sigma-Aldrich) at 1 wt% in DI water.

5.3. Spinal cord scaffold construction

The spinal cord scaffolds consisted of a soft MAC hydrogel within an outer conduit of MAC, similar to previous reports.^[16, 20] To form them, we first synthesized the outer MAC conduits, then prepared the hydrogel solution, and finally filled the conduits with hydrogel and photocrosslinked them. We cultured the scaffolds overnight in growth medium before

implanting into subcutaneous tissue. All scaffolds in this study contained immobilized IFN- γ .

Outer MAC conduit: we made hollow MAC tubes similar to previously reported techniques.^[20, 42] Briefly, we dissolved MAC at 3 wt% in DI water before mixing it with an equal volume of 200 proof ethanol at 4 °C for 1 h. We then added 75 μL acetic anhydride (EMD) per 5 mL MAC:EtOH solution and immediately added it to a mold.^[20] We then let the tube air dry overnight at RT, rehydrated it in DI water, washed 3x with DI water, and cut the long tube of MAC into 1 cm long tubes. We sterilized the tubes in 70% EtOH overnight, and then washed them in DI water before proceeding.

Internal hydrogel: We dissolved lyophilized MAC-DIBO in DI water to form a 3 wt% solution, and autoclaved it prior to use. The final hydrogel included the following components: photo-reactive laminin (50 μg per g final hydrogel solution), photoinitiator (final concentration 0.2 wt%), azide-tagged IFN- γ (600 ng/g final solution), and NSCs in growth medium (3×10^6 cells/g final solution, chosen based on prior work).^[16, 20] For the no NSC groups, we added growth medium without NSCs. We adjusted the final volume with 10X PBS to obtain a 2 wt% solution of MAC-DIBO. To form the solution, we first added an appropriate amount of IFN- γ and 10X PBS to the 3 wt% MAC-DIBO solution and allowed it to react for 1h at 4 °C (enabling immobilization of IFN- γ via strain-promoted click). We then added the remaining components and mixed the solution in a dual asymmetric centrifugal mixer (1.5 m, 1500 RPM; SpeedMixer DAC 150 FVZ, Hauschild Engineering).

Final scaffold construction: We placed the individual MAC tubes into 24 well plates. Into each tube, we pipetted 150–200 μL of hydrogel solution. We then crosslinked them via UV light exposure (23 mW/cm² for 40s, IntelliRay 400, UVitron). We then added NSC growth media and cultured the scaffolds overnight (37 °C, 5% CO₂) with 2 media changes.

5.4. Subcutaneous implantation of spinal cord scaffolds

All surgical procedures were performed aseptically. For groups receiving subcutaneously matured scaffolds, we implanted them for maturation as previously described,^[19, 20] with minor modifications. Briefly, we anesthetized (via isoflurane) the animals (8 wk old female Fisher 344, Envigo) and prepped the surgical site. We made 1 incision in the thoracic region (approx. T5, 3–5 cm left of the midline) and implanted 2 scaffolds (in the same incision, for redundancy) per rat in a pocket of subcutaneous tissue. After closing the incision with Michel clips, we allowed the animals to recover, administering carprofen (3 days post-op, 5 mg/kg) as an analgesic. We started with 8 animals per group. Following subcutaneous implantation of the scaffolds, we allowed the rats to recover for 2 wks (Figure 1) before proceeding with the hemisection injury. For the duration of this study, all rats were housed with cage mates.

5.5. Hemisection SCI model

We performed the hemisection similar to previous reports.^[16] After anesthetizing (via isoflurane) the rats (10 wk old female Fisher 344, Envigo) and preparing the surgical site, we made an incision along the midline. We then exposed the dorsal processes from T8-T11 and

exposed the spinal cord under T10 via laminectomy. For injury animals (all groups aside from laminectomy only), we performed a right lateral hemisection at T10 with a #11 scalpel blade, removing 2 mm of the cord and taking care to ensure that no neuronal connections remained on the right side. We controlled bleeding as necessary using Gelfoam (Pfizer). After achieving hemostasis, we closed the muscle with 4–0 Vicryl (Ethicon) sutures and the skin with Michel clips. We provided subcutaneous carprofen as an analgesic (3 days post-op, 5 mg/kg), along with subcutaneous saline (5, 5, 4, 3, 2 mL/rat/day, respectively, over 5 days post-op). We expressed bladders twice daily until the normal reflex returned, monitoring for signs of bladder infection. In cases of bladder infection (1/80 rats total), we administered enrofloxacin (10 mg/kg, twice daily subcutaneously) for 1 week. Any rats which rapidly lost weight, failed to regain normal voiding reflex after 4 wks, or showed signs of persistent infection were euthanized (7 rats total, resulting in n = 7 or 8 for functional outcome measures). We allowed the rats to recover for 2 wks prior to implantation (non-subcutaneously matured scaffolds) or transplantation (groups with subcutaneously matured scaffolds) surgeries (Figure 1). Importantly, a laminectomy only group (Figure A.8) showed no deficits (BBB = 21), indicating that our surgical technique did not cause unintended injury.

5.6. ISP administration

We administered ISP (synthesized by GenScript) to ISP+ groups as previously described.^[8] We prepared a 5 μ M solution in sterile DMSO:saline (1:20) and injected 500 μ L subcutaneously, once daily. ISP administration began 1 day post-op and continued throughout the duration of the study.

5.7. Creation of MAC films

In order to hold the scaffolds in place following placement into the lesion site, we drew inspiration from previously published reports^[43] and used a thin film made of dried MAC. To prepare it, we dissolved MAC at 2 wt% in DI water, autoclaved it, and poured it onto a sterile sheet of polytetrafluoroethylene (autoclaved). We allowed this to dry overnight in a laminar flow hood and then peeled the MAC film from the surface. We kept the films sterile until use.

5.8. Placement of scaffolds into lesion

After allowing the animals to recover for 2 wks following their hemisection, we inserted (either via transplantation for the subcutaneously matured groups, or implantation for the remaining groups) the scaffolds into the spinal cord lesion. First, we anesthetized (via isoflurane) the animals and prepared the surgical site. We then reopened the incision from the injury surgery and located T10. Carefully, we removed scar tissue until the entire lesion was clearly visible. We controlled bleeding as necessary using Gelfoam (Pfizer). For the subcutaneously matured scaffolds, we reopened the pocket into which the scaffolds were implanted 4 weeks prior located by massaging the skin until the scaffold was located, removed them, and carefully cut one of the scaffolds to match the hemisection geometry (i.e., into a half-cylinder). We qualitatively observed that the scaffolds had largely maintained their starting geometry and gross mechanical properties. We did not observe any degradation or erosion of the outer MAC conduit. For the non-subcutaneously matured

groups, we removed the scaffold from the 24 well plate and cut it to match the hemisection geometry. Next, we carefully placed the scaffold into the lesion and held it in place with a small, circular piece of MAC film (prepared as described above). Finally, we sutured the muscle closed with 4–0 Vicryl and closed the skin with Michel clips. The animals recovered as described above, with the same analgesia and saline administration. None of the animals which had previously regained bladder function lost it following this surgery, and no rats experienced additional complications. We monitored recovery for 16 wks following scaffold placement.

5.9. BBB testing

BBB analysis was performed as described in.^[44] Briefly, 2 trained observers watched each rat explore an open-field arena for 4 minutes. One of the experimenters recorded the observations of both. We collected scores weekly.

5.10. Gait analysis

To obtain quantitative data regarding locomotor recovery following their injury, we used an open-source gait technique: gait analysis instrumentation and technology optimized for rodents (GAITOR). Details regarding the equipment, procedure, and data analysis can be found in.^[22, 21] Briefly, we took high-speed footage of each rat walking back and forth across a closed arena (5–7 videos per rat) at 2 wk intervals, beginning at 4 wks following scaffold insertion. We analyzed this footage via automated gait analysis through hues and areas (AGATHA, a software component of GAITOR) and extracted spatial (i.e., where they placed each paw) and temporal (i.e., when each placement occurred, and for how long) information. We then used this information to calculate relevant gait parameters: duty factor (how long each paw is in contact with the floor, expressed as % of total gait cycle) and paw placement accuracy (distance between ipsilateral fore and hindpaw centroids). Here, we report duty factor imbalance (right duty factor — left duty factor) for fore and hindlimb pairs, and paw placement accuracy for left and right limb pairs. As paw placement accuracy is dependent on walking speed, we calculated its residual (vs. a pool of nave data collected from age- and weight-matched Fisher 344s). As before,^[21] our injury model affected hindlimb duty factor imbalance and right paw placement accuracy, but not forelimb duty factor imbalance or left paw placement accuracy. Thus, we use hindlimb duty factor imbalance and right paw placement accuracy as measures of locomotor recovery following injury and report forelimb duty factor imbalance and left paw placement accuracy as supporting data (Figure A.10) to show that our injury model was specific for right hindlimb control.

5.11. Retrograde tracer administration

We performed retrograde tracing (FluoroGold, FluoroChrome) as described in^[16, 45] with no deviations. We administered the tracer at wk 15 and allowed the rats to recover for 1 wk before sacrifice.

5.12. Tissue preparation for tracer and IHC analysis

At 16 wks post scaffold placement, we euthanized the rats (after terminal anesthetization) via paraformaldehyde (PFA, 4% in PBS) perfusion. We then carefully explanted the entire spinal cord and post-fixed them in 4% PFA at 4 °C overnight. Next, we separated the cord into two segments: first, T8-T13 (containing the lesion and scaffold) was separated from the cord and placed into 70% EtOH for paraffin embedding and sectioning (used in IHC analysis). Second, T5-T8 was separated from the cord, placed into 0.2 M phosphate buffer at 4 °C overnight, and then transferred to 30% sucrose for 3 days (also 4 °C) prior to cryosectioning and tracer analysis.

5.13. Retrograde tracer analysis

We analyzed the retrograde tracer uptake of all animals (n = 7 or 8). Segments for tracer analysis were embedded in OCT Compound (Tissue-Tek) and stored at -80 °C until cryosectioning (Leica CM 1850). We collected 25 μ m cross sections from T5-T8 and imaged (DAPI channel, using identical acquisition settings) each section (Olympus IX81) to determine relative tracer intensity as follows: we applied an identical threshold to each image and counted the total number of bright (above the threshold) pixels within a region of interest (consistently-sized) on each side of the cord (left and right). We then took the ratio of right/left, controlling for overall uptake of tracer between each animal. This analysis was automated in MATLAB (Mathworks).

5.14. IHC analysis

For IHC analysis, we chose 4 rats (out of 8 total) from each group at random. We embedded spinal cords in paraffin and sectioned them longitudinally (top-down, 10 μ m sections). We deparaffined each slide by immersion in the following solutions, in order: 100% xylenes (Fisher) for 5 min (2x), 100% ethanol (Fisher) for 3 min (2x) 95% ethanol for 3 min, and then 70% ethanol for 3 min, followed by rinsing in cold tap water. We performed heat-induced antigen retrieval by autoclaving the slides for 10m in tris-EDTA buffer (10 mM tris base, 1mM EDTA, 0.05% Tween-20, pH 9.0 - all Sigma) prior to staining. We conducted IHC as previously described,^[13, 20] with the following primary antibodies: RIP (DSHB, 1:5 dilution), nestin (DSHB, 1:20 dilution), neurofilament (Millipore, 1:400 dilution), and NeuN (Millipore, 1:500 dilution). For secondary antibodies, we used either Cy3-conjugated anti-rabbit (Millipore, 1:400 dilution) or Cy5-conjugated anti-mouse (SCBT, 1:50 dilution). Images were collected on an Olympus FV1000 confocal microscope. To count the total number of GFP+ cells in each section, we collected images of the gel at 10X magnification in random locations throughout the gel. We then manually applied a threshold and used the analyze particles feature within ImageJ. To determine the distribution of GFP+ cell lineage (% NeuN+ and nestin+), we collected images within the gel at 20X in random locations and manually counted the number of GFP+ cells and the number of NeuN or nestin+/GFP+ cells. n = 4 was used for all IHC analyses.

5.15. Experimental design and statistical analysis

Our primary hypothesis was that subcutaneous maturation combined with ISP would improve locomotor recovery over a period of 16 weeks following placement of scaffolds into

the lesion when compared to a no treatment control. For measurements conducted over time (BBB score, gait parameters), we tested this hypothesis using a repeated measures analysis of variance (ANOVA, time as within-subjects variable) with Tukey's *post-hoc*. For endpoint measurements (retrograde tracing, IHC) we tested it using an ANOVA with Tukey's *post-hoc*. For the repeated measures tests, groups which were significantly different from the no treatment control at each timepoint are indicated by various symbols (&, etc.) as indicated in each legend. For the ANOVAs, we indicated significant differences using letters (groups not sharing a letter are different) or *, as indicated on each graph and within the figure caption. For all tests, $p < 0.05$ was considered to be significant. Statistical analysis was conducted in either MATLAB (MathWorks), SAS 9.4 (SAS Institute), or GraphPad Prism 6 (GraphPad Software).

Supplementary Material

Refer to Web version on PubMed Central for supplementary material.

Acknowledgments

This work was supported by the National Institute of Neurological Disorders and Stroke (R21NS096571-01). Funding for the Rat Resource & Research Center was provided by grant P40OD011062. Additionally, the authors thank Dr. Hossein Tavana (UA) for the use of his cryostat and Ms. Eleanor Plaster for her assistance with sample preparation for IHC. Lastly, TRH and NDJ thank the faculty at the Ohio State University Spinal Cord Injury Training Program (sponsored by the Craig H. Neilsen Foundation) for providing training (in both surgical technique and BBB testing) and advice.

References

- [1]. Silva NA, Sousa N, Reis RL, Salgado AJ, From basics to clinical: a comprehensive review on spinal cord injury, *Prog Neurobiol* 114 (2014) 25–57. doi:10.1016/j.pneurobio.2013.11.002. [PubMed: 24269804]
- [2]. Sabelstrom H, Stenudd M, Frisen J, Neural stem cells in the adult spinal cord, *Exp Neurol* 260 (2014) 44–9. doi:10.1016/j.expneurol.2013.01.026. [PubMed: 23376590]
- [3]. Ham TR, Leipzig ND, Biomaterial strategies for limiting the impact of secondary events following spinal cord injury, *Biomed Mater* 13 (2) (2018) 024105. doi:10.1088/1748-605X/aa9bbb. [PubMed: 29155409]
- [4]. Fenrich KK, May Z, Torres-Espin A, Forero J, Bennett DJ, Fouad K, Single pellet grasping following cervical spinal cord injury in adult rat using an automated full-time training robot, *Behav Brain Res* 299 (2016) 59–71. doi:10.1016/j.bbr.2015.11.020. [PubMed: 26611563]
- [5]. Field-Fote EC, Yang JF, Basso DM, Gorassini MA, Supraspinal control predicts locomotor function and forecasts responsiveness to training after spinal cord injury, *J Neurotrauma* 34 (9) (2017) 1813–1825. doi:10.1089/neu.2016.4565. [PubMed: 27673569]
- [6]. Harkema S, Gerasimenko Y, Hodes J, Burdick J, Angeli C, Chen Y, Ferreira C, Willhite A, Rejc E, Grossman RG, Edgerton VR, Effect of epidural stimulation of the lumbosacral spinal cord on voluntary movement, standing, and assisted stepping after motor complete paraplegia: a case study, *Lancet* 377 (9781) (2011) 1938–47. doi:10.1016/S0140-6736(11)60547-3. [PubMed: 21601270]
- [7]. Ichiyama RM, Gerasimenko YP, Zhong H, Roy RR, Edgerton VR, Hindlimb stepping movements in complete spinal rats induced by epidural spinal cord stimulation, *Neurosci Lett* 383 (3) (2005) 339–44. doi:10.1016/j.neulet.2005.04.049. [PubMed: 15878636]
- [8]. Lang BT, Cregg JM, DePaul MA, Tran AP, Xu K, Dyck SM, Madalena KM, Brown BP, Weng Y, Li S, Karimi-Abdolrezaee S, Busch SA, Shen Y, Silver J, Modulation of the proteoglycan receptor ptpsigma promotes recovery after spinal cord injury, *Nature* doi:10.1038/nature13974.

- [9]. Mothe AJ, Tator CH, Review of transplantation of neural stem/progenitor cells for spinal cord injury, *Int J Dev Neurosci* 31 (7) (2013) 701–13. doi:10.1016/j.ijdevneu.2013.07.004. [PubMed: 23928260]
- [10]. Lu P, Jones LL, Snyder EY, Tuszynski MH, Neural stem cells constitutively secrete neurotrophic factors and promote extensive host axonal growth after spinal cord injury, *Experimental Neurology* 181 (2) (2003) 115–129. doi:10.1016/s0014-4886(03)00037-2. [PubMed: 12781986]
- [11]. Hwang DH, Shin HY, Kwon MJ, Choi JY, Ryu BY, Kim BG, Survival of neural stem cell grafts in the lesioned spinal cord is enhanced by a combination of treadmill locomotor training via insulin-like growth factor-1 signaling, *J Neurosci* 34 (38) (2014) 12788–800. doi:10.1523/JNEUROSCI.5359-13.2014. [PubMed: 25232115]
- [12]. Lu P, Wang Y, Graham L, McHale K, Gao M, Wu D, Brock J, Blesch A, Rosenzweig ES, Havton LA, Zheng B, Conner JM, Marsala M, Tuszynski MH, Long-distance growth and connectivity of neural stem cells after severe spinal cord injury, *Cell* 150 (6) (2012) 1264–73. doi:10.1016/j.cell.2012.08.020. [PubMed: 22980985]
- [13]. Ham TR, Farrag M, Leipzig ND, Covalent growth factor tethering to direct neural stem cell differentiation and self-organization, *Acta Biomater* doi:10.1016/j.actbio.2017.01.068.
- [14]. Leipzig ND, Xu C, Zahir T, Shoichet MS, Functional immobilization of interferon-gamma induces neuronal differentiation of neural stem cells, *J Biomed Mater Res A* 93 (2) (2010) 625–33. doi:10.1002/jbm.a.32573. [PubMed: 19591237]
- [15]. Leipzig ND, Shoichet MS, The effect of substrate stiffness on adult neural stem cell behavior, *Biomaterials* 30 (36) (2009) 6867–78. doi:10.1016/j.biomaterials.2009.09.002. [PubMed: 19775749]
- [16]. Li H, Ham TR, Neill N, Farrag M, Mohrman AE, Koenig AM, Leipzig ND, A hydrogel bridge incorporating immobilized growth factors and neural stem/progenitor cells to treat spinal cord injury, *Advanced Healthcare Materials* 5 (7) (2016) 802–812. doi:10.1002/adhm.201500810. [PubMed: 26913590]
- [17]. Lu P, Ceto S, Wang Y, Graham L, Wu D, Kumamaru H, Staufenberg E, Tuszynski MH, Prolonged human neural stem cell maturation supports recovery in injured rodent CNS, *J Clin Invest* 127 (9) (2017) 3287–3299. doi:10.1172/JCI92955. [PubMed: 28825600]
- [18]. Tataru AM, Wong ME, Mikos AG, In vivo bioreactors for mandibular reconstruction, *J Dent Res* 93 (12) (2014) 1196–202. doi:10.1177/0022034514547763. [PubMed: 25139360]
- [19]. Farrag M, Leipzig ND, Subcutaneous maturation of neural stem cell-loaded hydrogels forms region-specific neuroepithelium, *Cells* 7 (10). doi:10.3390/cells7100173.
- [20]. Li H, Koenig AM, Sloan P, Leipzig ND, In vivo assessment of guided neural stem cell differentiation in growth factor immobilized chitosan-based hydrogel scaffolds, *Biomaterials* 35 (33) (2014) 9049–57. doi:10.1016/j.biomaterials.2014.07.038. [PubMed: 25112933]
- [21]. Ham TR, Farrag M, Soltisz AM, Lakes EH, Allen KD, Leipzig ND, Automated gait analysis detects improvements after intracellular sigma peptide administration in a rat hemisection model of spinal cord injury, *Ann Biomed Eng* 47 (3) (2019) 744–753. doi:10.1007/s10439-019-02198-0. [PubMed: 30627839]
- [22]. Jacobs BY, Lakes EH, Reiter AJ, Lake SP, Ham TR, Leipzig ND, Porvasnik SL, Schmidt CE, Wachs RA, Allen KD, The open source gaitor suite for rodent gait analysis, *Scientific Reports* 8 (1) (2018) 9797. doi:10.1038/s41598-018-28134-1. [PubMed: 29955094]
- [23]. Kloefkorn HE, Pettengill TR, Turner SM, Streeter KA, Gonzalez-Rothi EJ, Fuller DD, Allen KD, Automated gait analysis through hues and areas (agatha): A method to characterize the spatiotemporal pattern of rat gait, *Ann Biomed Eng* 45 (3) (2016) 711–25. doi:10.1007/s10439-016-1717-0. [PubMed: 27554674]
- [24]. Li H, Wijekoon A, Leipzig ND, 3d differentiation of neural stem cells in macroporous photopolymerizable hydrogel scaffolds, *PLoS One* 7 (11) (2012) e48824. doi:10.1371/journal.pone.0048824. [PubMed: 23144988]
- [25]. Wilkinson AE, Kobelt LJ, Leipzig ND, Immobilized ECM molecules and the effects of concentration and surface type on the control of NSC differentiation, *Journal of Biomedical Materials Research Part A* 102 (10) (2014) 3419–3428. doi:10.1002/jbm.a.35001. [PubMed: 24133022]

- [26]. Leipzig ND, Wylie RG, Kim H, Shoichet MS, Differentiation of neural stem cells in three-dimensional growth factor-immobilized chitosan hydrogel scaffolds, *Biomaterials* 32 (1) (2011) 57–64. doi:10.1016/j.biomaterials.2010.09.031. [PubMed: 20934216]
- [27]. Lu P, Woodru G, Wang Y, Graham L, Hunt M, Wu D, Boehle E, Ahmad R, Poplawski G, Brock J, Goldstein LS, Tuszynski MH, Long-distance axonal growth from human induced pluripotent stem cells after spinal cord injury, *Neuron* 83 (4) (2014) 789–96. doi:10.1016/j.neuron.2014.07.014. [PubMed: 25123310]
- [28]. Yang Y, De Laporte L, Zelivyanskaya ML, Whittlesey KJ, Anderson AJ, Cummings BJ, Shea LD, Multiple channel bridges for spinal cord injury: Cellular characterization of host response, *Tissue Engineering Part A* 15 (11) (2009) 3283–3295. doi:DOI10.1089/ten.tea.2009.0081. [PubMed: 19382871]
- [29]. Moore MJ, Friedman JA, Lewellyn EB, Mantila SM, Krych AJ, Ameenuddin S, Knight AM, Lu L, Currier BL, Spinner RJ, Marsh RW, Windebank AJ, Yaszemski MJ, Multiple-channel scaffolds to promote spinal cord axon regeneration, *Biomaterials* 27 (3) (2006) 419–29. doi: S0142-9612(05)00707-6[pil]10.1016/j.biomaterials.2005.07.045 [PubMed: 16137759]
- [30]. Alluin O, Delivet-Mongrain H, Gauthier MK, Fehlings MG, Rossignol S, Karimi-Abdolrezaee S, Examination of the combined effects of chondroitinase abc, growth factors and locomotor training following compressive spinal cord injury on neuroanatomical plasticity and kinematics, *PLoS One* 9 (10) (2014) e111072. doi:10.1371/journal.pone.0111072. [PubMed: 25350665]
- [31]. Fuhrmann T, Anandakumaran PN, Shoichet MS, Combinatorial therapies after spinal cord injury: How can biomaterials help?, *Adv Healthc Mater* 6 (10). doi:10.1002/adhm.201601130.
- [32]. Tsukamoto A, Uchida N, Capela A, Gorba T, Huhn S, Clinical translation of human neural stem cells, *Stem Cell Res Ther* 4 (4) (2013) 102. doi:10.1186/srct313 [PubMed: 23987648]
- [33]. Ogawa D, Okada Y, Nakamura M, Kanemura Y, Okano HJ, Matsuzaki Y, Shimazaki T, Ito M, Ikeda E, Tamiya T, Nagao S, Okano H, Evaluation of human fetal neural stem/progenitor cells as a source for cell replacement therapy for neurological disorders: properties and tumorigenicity after long-term in vitro maintenance, *J Neurosci Res* 87 (2) (2009) 307–17. doi:10.1002/jnr.21843. [PubMed: 18972448]
- [34]. Piltti KM, Salazar DL, Uchida N, Cummings BJ, Anderson AJ, Safety of human neural stem cell transplantation in chronic spinal cord injury, *Stem Cells Transl Med* 2 (12) (2013) 961–74. doi:10.5966/sctm.2013-0064. [PubMed: 24191264]
- [35]. Shoakazemi A, Flannery T, McConnell RS, Long-term outcome of subcutaneously preserved autologous cranioplasty, *Neurosurgery* 65 (3) (2009) 505–10; discussion 510. doi:10.1227/01.NEU.0000350870.69891.86. [PubMed: 19687696]
- [36]. Movassaghi K, Ver Halen J, Ganchi P, Amin-Hanjani S, Mesa J, Yarem-chuk MJ, Cranioplasty with subcutaneously preserved autologous bone grafts, *Plast Reconstr Surg* 117 (1) (2006) 202–6. doi:10.1097/01.prs.0000187152.48402.17. [PubMed: 16404268]
- [37]. Caplan AI, Correa D, The msc: an injury drugstore, *Cell Stem Cell* 9 (1) (2011) 11–5. doi:10.1016/j.stem.2011.06.008. [PubMed: 21726829]
- [38]. Caplan AI, Mesenchymal stem cells: Time to change the name!, *Stem Cells Transl Med* 6 (6) (2017) 1445–1451. doi:10.1002/sctm.17-0051. [PubMed: 28452204]
- [39]. Amado LC, Saliaris AP, Schuleri KH, St John M, Xie JS, Cat-taneo S, Durand DJ, Fitton T, Kuang JQ, Stewart G, Lehrke S, Baumgartner WW, Martin BJ, Heldman AW, Hare JM, Cardiac repair with intramyocardial injection of allogeneic mesenchymal stem cells after myocardial infarction, *Proc Natl Acad Sci U S A* 102 (32) (2005) 11474–9. doi:10.1073/pnas.0504388102. [PubMed: 16061805]
- [40]. McCormick AM, Jarmusik NA, Endrizzi EJ, Leipzig ND, Expression, isolation, and purification of soluble and insoluble biotinylated proteins for nerve tissue regeneration, *J Vis Exp* (83) (2014) e51295. doi:10.3791/51295.
- [41]. McCormick AM, Wijekoon A, Leipzig ND, Specific immobilization of biotinylated fusion proteins ngf and sema3a utilizing a photo-cross-linkable di-azirine compound for controlling neurite extension, *Bioconj Chem* 24 (9) (2013) 1515–26. doi:10.1021/bc400058n. [PubMed: 23909702]

- [42]. Freier T, Montenegro R, Shan Koh H, Shoichet MS, Chitin-based tubes for tissue engineering in the nervous system, *Biomaterials* 26 (22) (2005) 4624–32. [PubMed: 15722132]
- [43]. Gunther MI, Weidner N, Muller R, Blesch A, Cell-seeded alginate hydrogel scaffolds promote directed linear axonal regeneration in the injured rat spinal cord, *Acta Biomater* 27 (2015) 140–150. doi:10.1016/j.actbio.2015.09.001. [PubMed: 26348141]
- [44]. Basso DM, Beattie MS, Bresnahan JC, A sensitive and reliable locomotor rating scale for open field testing in rats, *J Neurotrauma* 12 (1) (1995) 1–21. [PubMed: 7783230]
- [45]. Tsai EC, van Bendegem RL, Hwang SW, Tator CH, A novel method for simultaneous anterograde and retrograde labeling of spinal cord motor tracts in the same animal, *J Histochem Cytochem* 49 (9) (2001) 1111–22. doi:10.1177/002215540104900905. [PubMed: 11511680]

Author Manuscript

Author Manuscript

Author Manuscript

Author Manuscript

Highlights

- We have developed a methodology for synthesizing spinal cord bridges, consisting of a polysaccharide-based hydrogel, an immobilized engineered protein to specify stem cell differentiation, and neural stem cells, to aid in regeneration
- We report an approach to mature these bridges within the subcutaneous tissue prior to transplantation into injured rat spinal cords to improve integration and functional outcomes, which we confirmed via histology
- Priming spinal cord bridges in the subcutaneous environment is a relatively understudied approach, one which we show has the potential to improve their regenerative capacity

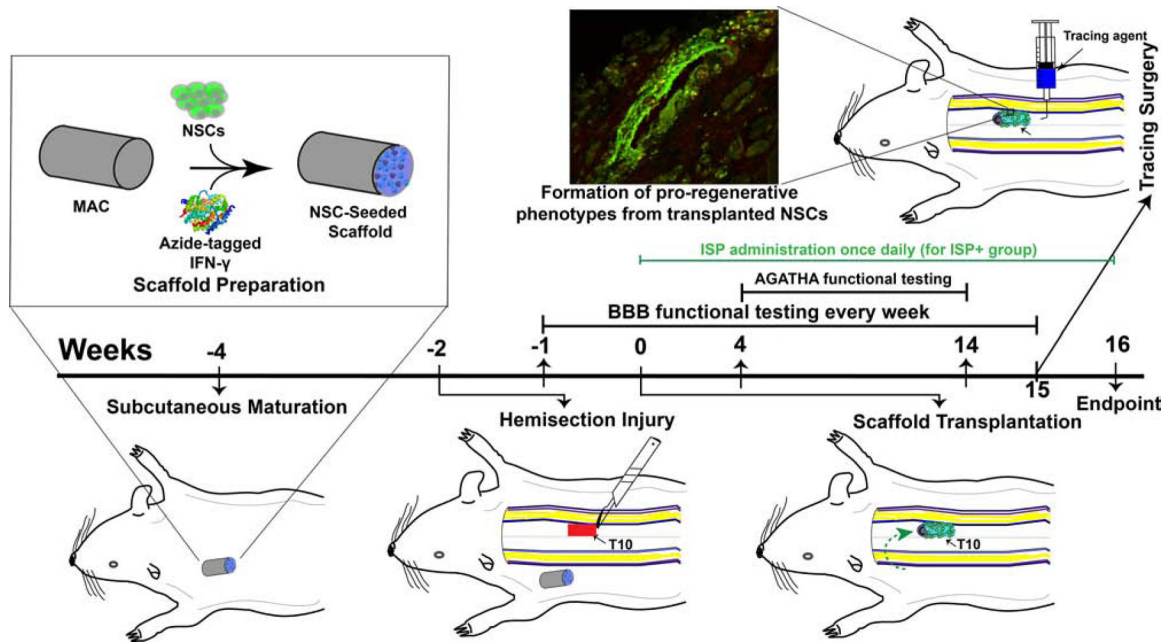


Figure 1:

Overview of current study. First, we formed NSC-seeded scaffolds from MAC and immobilized IFN- γ . We implanted them into subcutaneous tissue (in the thoracic region) and allowed them to mature for 4 weeks total (weeks -4 to 0). Two weeks later (week -2), we performed a right lateral T10 hemisection. We allowed the rats to recover for 2 weeks before transplanting the scaffolds from the subcutaneous environment (or implanting them directly for non-matured controls, week 0). We then monitored locomotor recovery over 16 weeks before performing tissue-level analyses (week 16).

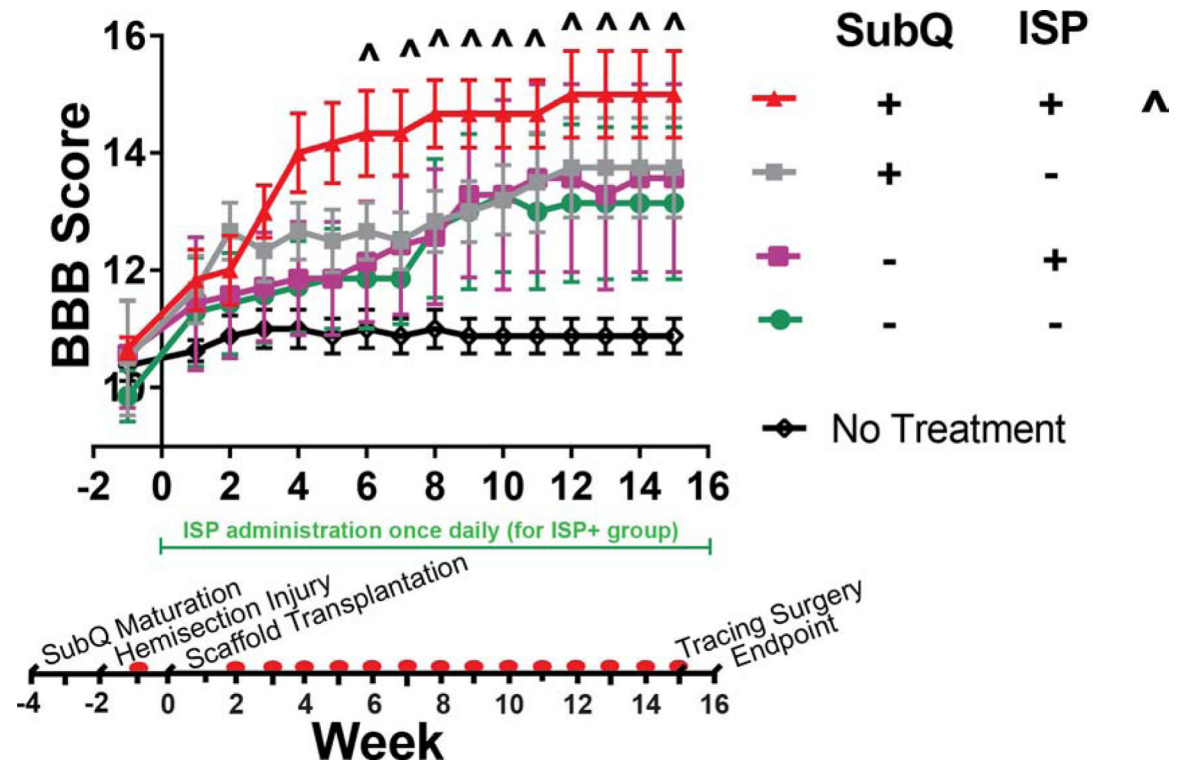


Figure 2:

Subcutaneous maturation in combination with ISP administration contributes to improved BBB scores. Without ISP, we found that subcutaneously maturing NSC-seeded scaffolds improved scores, but without statistical significance vs. the no treatment control ($p > 0.05$). Likewise, implanting non-matured scaffolds improved recovery, but not to the level of the subcutaneously matured NSC scaffolds. With ISP and subcutaneous maturation together, we observed a statistically significant improvement vs. no treatment control beginning at week 6 ($p < 0.05$). All data points are mean \pm SEM, $n = 7$ or 8 . Symbols (^) indicate which groups are statistically different from the no treatment control at each week. Significance determined by repeated measures ANOVA ($\alpha = 0.05$, time is within-subjects variable) and Tukey's *post-hoc*. Red dots on timeline indicate collection of BBB data.

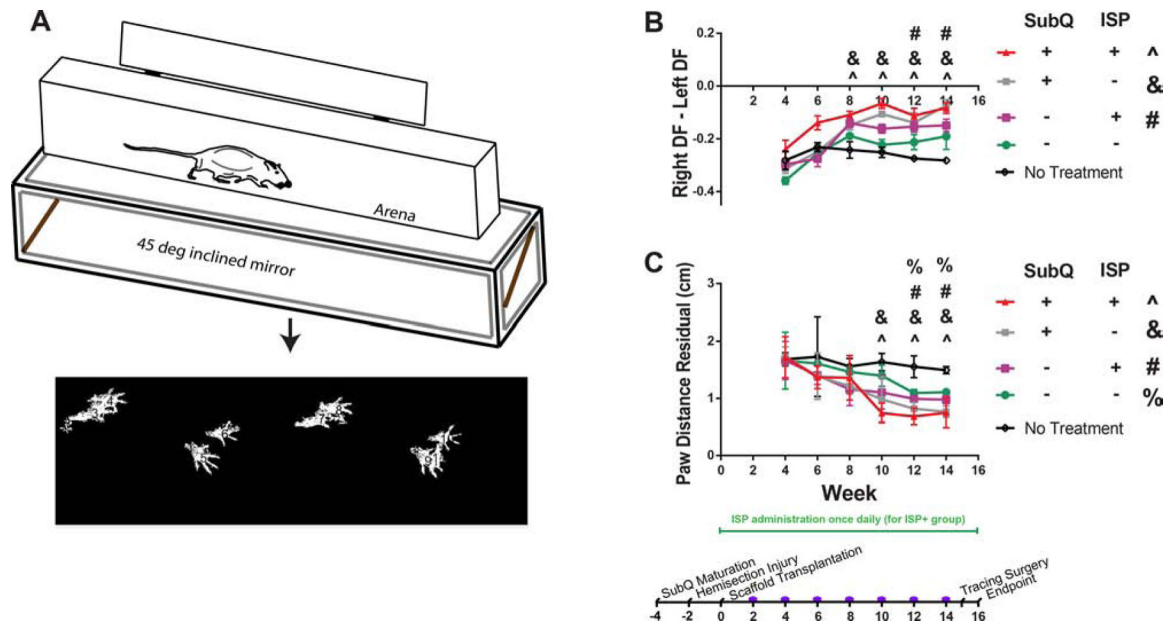


Figure 3:

Subcutaneous maturation, ISP administration, and NSCs all contributed to improved gait parameters as measured by GAITOR.^[22, 21] A: Brief schematic of the procedure for collecting gait data. More details on the arena used to collect videos and software used to extract gait data can be found in ref.^[22] Note the distance in overlap between right and left paws - this is reflected in paw distance residual. B: Hindlimb duty factor imbalance results. A negative value indicates that the left limb dominates. With ISP administration, both NSC-seeded scaffolds (with and without maturation) improved outcomes vs. control. C: Right paw placement accuracy results. The results are presented as velocity-weighted residuals. Without ISP administration, both NSC-seeded scaffolds improved outcomes vs. control, although subcutaneous maturation showed benefits at an earlier timepoint. Similarly, with ISP administration, both types of NSC-seeded scaffold improved outcomes as well, but the groups that received subcutaneously matured scaffolds showed improvements at an earlier timepoint. All data points are mean SEM, $n = 7$ or 8 . Symbols (e.g., \wedge , see figure legend) indicate which groups are statistically different \pm from the no treatment control at each week. Significance determined by repeated measures ANOVA ($\alpha = 0.05$, time is within-subjects variable) and Tukey's *post-hoc*. Purple dots on timeline indicate collection of gait data.

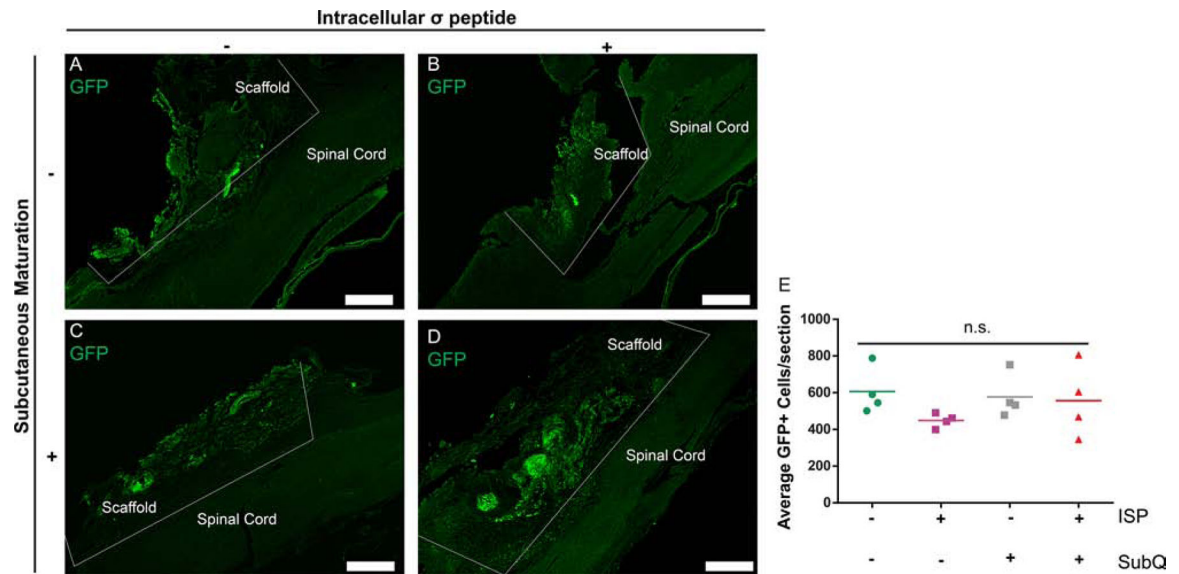


Figure 4:

Neither subcutaneous maturation nor ISP administration affects the number of remaining implanted cells. A-D: Images show similar numbers, distributions, and morphologies of implanted cells, with one key difference — the ellipsoid clusters of cells reflective of subcutaneous maturation seen in C + D. E: Quantifying the number of GFP+ cells remaining confirmed our observations. Scale bars = 500 μ m. Data are presented as scatter plots, n = 4. n.s. indicates p > 0.05, ANOVA.

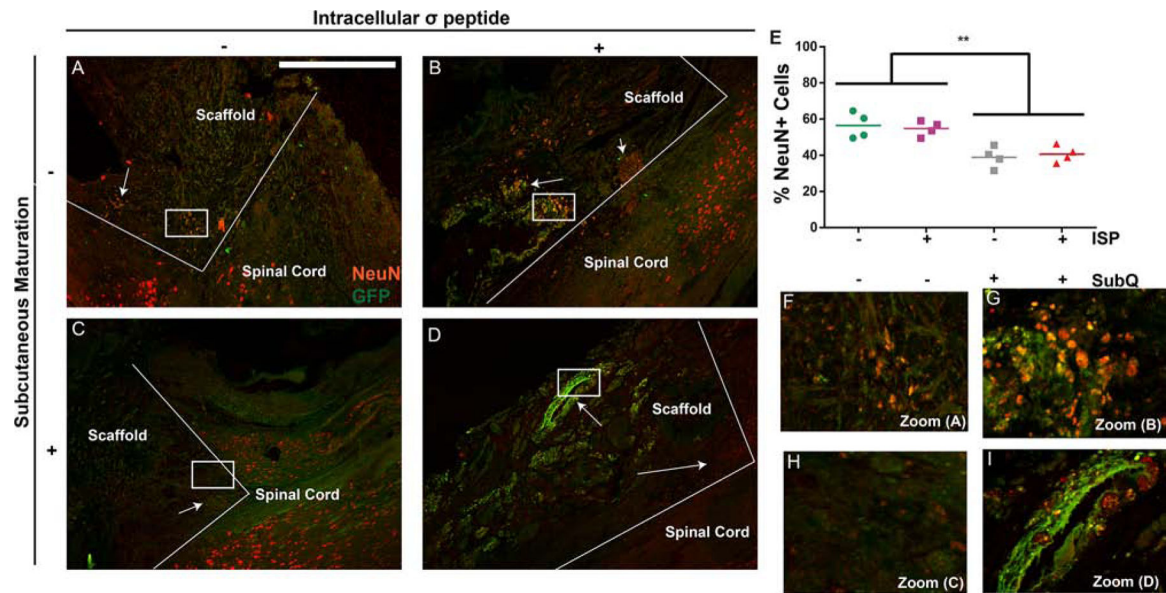


Figure 5:

Subcutaneous maturation, but not ISP, decreases neuronal differentiation of implanted cells. A-D: Comparing the number of NeuN/GFP+ (yellow) cells between the non-matured (A+B) and the subcutaneously matured (C+D) groups shows more NeuN+/GFP+ cells in the non-matured groups (arrows), indicating greater lineage commitment. In the ISP+ groups, NeuN expression from GFP- (host) cells can be observed at the interface between the scaffold and the tissue (arrows), which is mostly absent in the ISP- groups. D: The ellipsoid clusters of cells were again observed in the subcutaneous groups, primarily without NeuN expression (arrow). Scale bars = 500 μ m, boxes show location of zoom. E: Quantification of NeuN expression from GFP+ cells confirmed our observations. Data are presented as scatter plots, n = 4. ** indicates $p < 0.001$, ANOVA with Tukey's *post-hoc*, $\alpha = 0.05$. F-I: Zoomed-in versions of A-D.

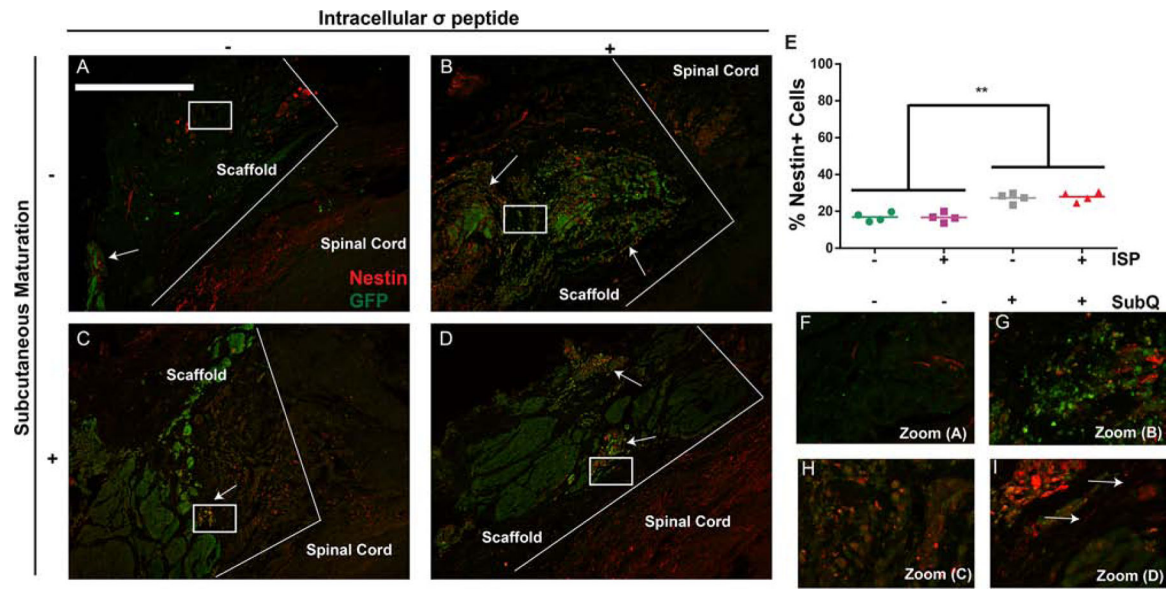


Figure 6:

Subcutaneous maturation, but not ISP, increases nestin expression from implanted cells. A-D We observed clear differences in the number of nestin/GFP+ (yellow) cells between groups receiving subcutaneous maturation vs. non-matured groups. Characteristic cell morphologies can be seen in all groups. Scale bars = 500 μ m, boxes show location of zoom. E: Quantification of nestin expression from GFP+ cells confirmed our observations. Data are presented as scatter plots, $n = 4$. ** indicates $p < 0.001$, ANOVA with Tukey's *post-hoc*, $\alpha = 0.05$. F-I: Zoomed-in versions of A-D. Importantly, aligned, nestin+ fibers can be seen in the group receiving subcutaneously matured NSC-seeded scaffolds with ISP (arrows), indicating a possible explanation for that group's increased BBB scores. These fibers were occasionally seen in the other groups, but not as consistently and without alignment.

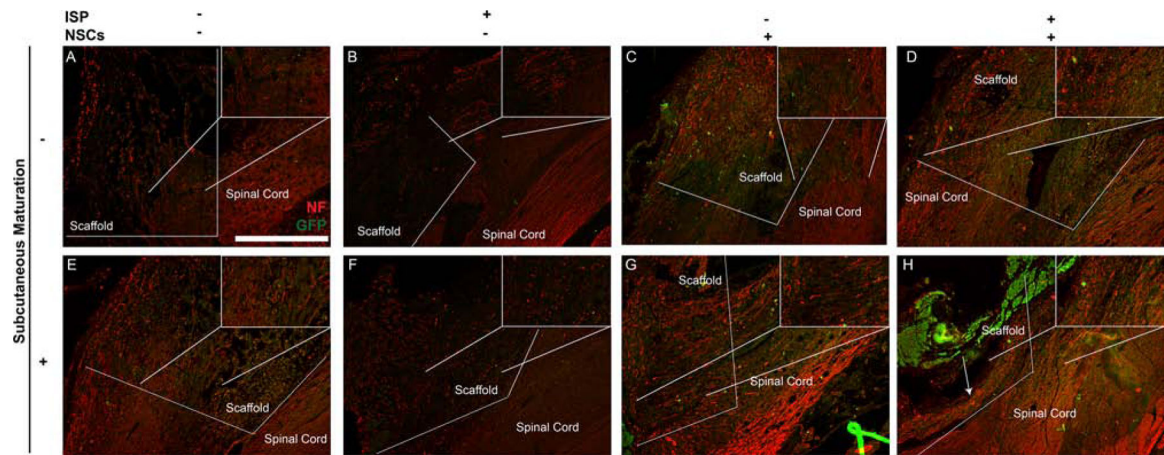


Figure 7:

Subcutaneous maturation with ISP administration increases neurofilament staining within the scaffolds. Magnified views of the interface between scaffold and tissue can be seen in insets within each image, indicated by a box and lines showing the zoom location. In all groups (A-H), some neurofilament staining was observed at the interface between the scaffold and the spinal cord, with NF+ fibers typically following the contours of the scaffold. As with the functional results, maturing empty scaffolds did not have an effect (A vs. E), while administering ISP to groups with empty scaffolds improved NF staining modestly (B + F vs. A + E). All groups receiving NSCs showed GFP+ cells within the scaffold: few had migrated into the surrounding cord. Importantly, the group receiving subcutaneously matured, NSC-seeded scaffolds with ISP treatment showed robust, aligned NF+ fibers throughout the scaffold (more detail in magnified inset). While these fibers failed to reconnect across the entire scaffold, they are similar in morphology and location to the nestin+ fibers observed in Figure 5, and do not co-stain for GFP. Scale bars = 500 μm .